

# **Supporting Information**

## **Nanostructured Surfaces of Opposite Charge from Self-Assembled Block Copolymers**

*Brandon A. Fultz<sup>¥</sup>, Tanguy Terlier<sup>‡</sup>, Beatriz Dunoyer de Segonzac<sup>¥</sup>, Rafael Verduzco<sup>\*£</sup>, and Justin G. Kennemur<sup>\*¥</sup>*

<sup>¥</sup> Department of Chemistry & Biochemistry, Florida State University, Tallahassee, FL 32306-4390, United States.

<sup>‡</sup> Department of Chemical and Biomolecular Engineering, Rice University, MS 362, 6100 Main Street, Houston, USA

<sup>\*</sup>SIMS laboratory, Shared Equipment Authority, Rice University, MS 126, 6100 Main Street, 77005 Houston Texas, United States.

### **Table of Contents:**

1. Additional characterization data.	p. S2
Figure S1.	Stacked $^1\text{H}$ NMR of CDPA, PtBMA, and PtBMA- <i>b</i> -P4VP.
Figure S2.	$^{13}\text{C}$ NMR of CDPA (RAFT CTA).
Figure S3.	ATR-IR spectrum of CDPA.
Figure S4.	$^{13}\text{C}$ NMR of PtBMA macro-CTA.
Figure S5.	ATR-IR spectrum of PtBMA macro-CTA.
Figure S6.	SEC trace of PtBMA macro-CTA.
Figure S7.	$^1\text{H}$ NMR of PtBMA- <i>b</i> -P4VP to determine segment molar ratios.
Figure S8.	$^{13}\text{C}$ NMR of PtBMA- <i>b</i> -P4VP.
Figure S9.	ATR-IR spectrum of PtBMA- <i>b</i> -P4VP.
Figure S10.	SEC trace of PtBMA- <i>b</i> -P4VP.
Figure S11.	DSC thermogram of PtBMA- <i>b</i> -P4VP.
Figure S12.	DSC thermogram of PtBMA macro-CTA.
Figure S13.	TGA thermogram of PtBMA- <i>b</i> -P4VP.
Figure S14.	ToF-SIMS spectrum of P4VP homopolymer in negative ion mode.
Figure S15.	ToF-SIMS spectrum of PtBMA homopolymer in negative ion mode.
Figure S16.	ToF-SIMS spectrum of P4VP homopolymer in positive ion mode.
Figure S17.	ToF-SIMS spectrum of PtBMA homopolymer in positive ion mode.
Figure S18.	ToF-SIMS imaging of dewetted film VP-MA(12-4)
2. Glass apparatus used for HCl vapor treatments	p. S13

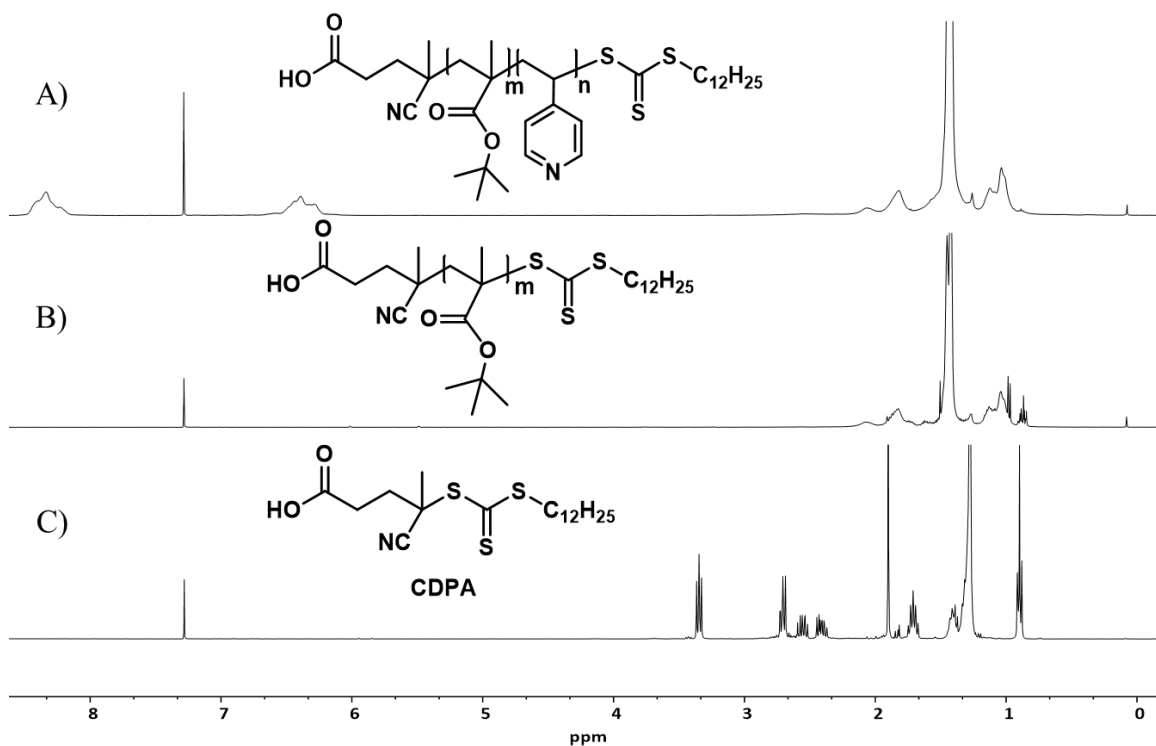


**Figure S1.** Stacked  $^1\text{H}$  NMR ( $\text{CDCl}_3$ , 25 °C) of A) P4VP-*b*-PtBMA, B) PtBMA homopolymer, and C) RAFT CTA (CDPA).

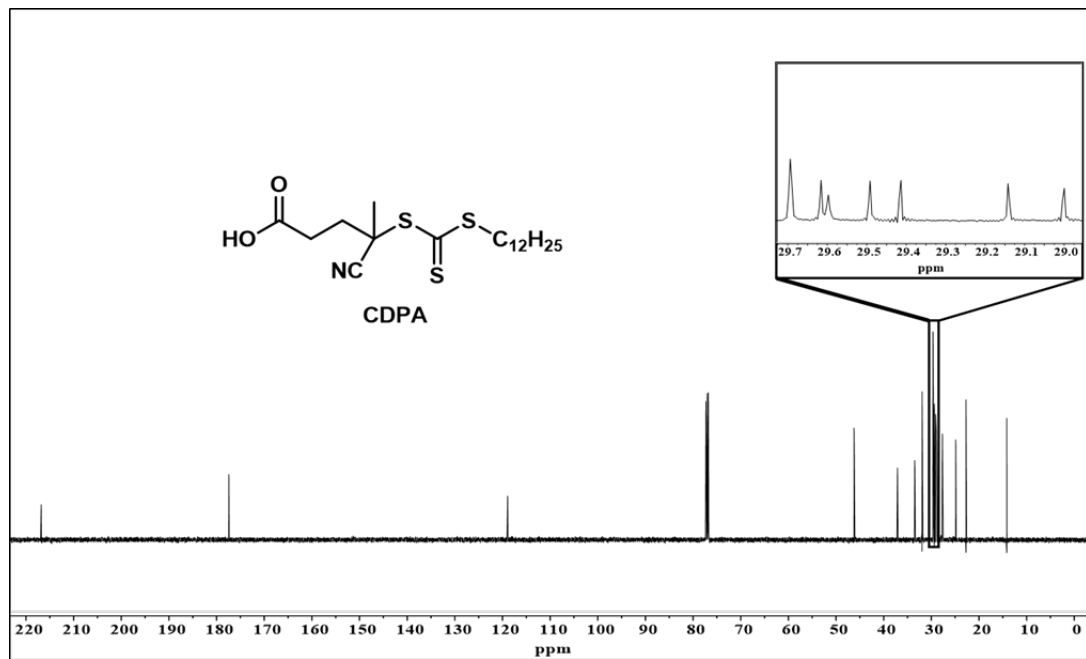


**Figure S2.**  $^{13}\text{C}$  NMR ( $\text{CDCl}_3$ , 25 °C, 125 MHz) of CDPA, RAFT CTA.

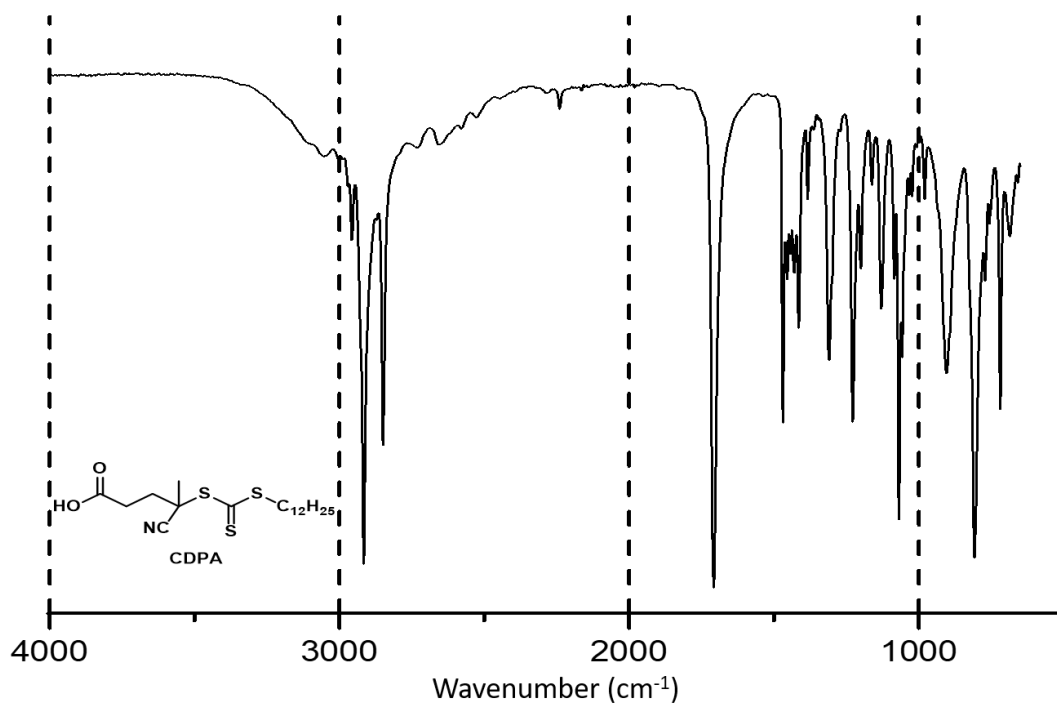


**Figure S3.** ATR-IR spectrum of CDPA, RAFT CTA, at 25 °C.

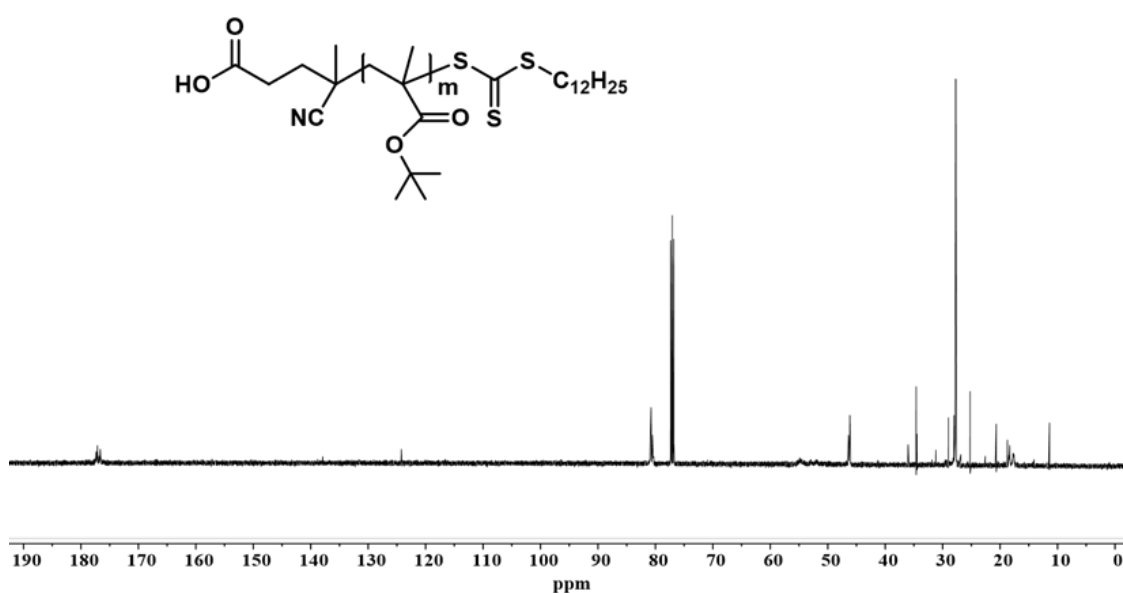


**Figure S4.** <sup>13</sup>C NMR (CDCl<sub>3</sub>, 25 °C, 125 MHz) of PtBMA macro-CTA.

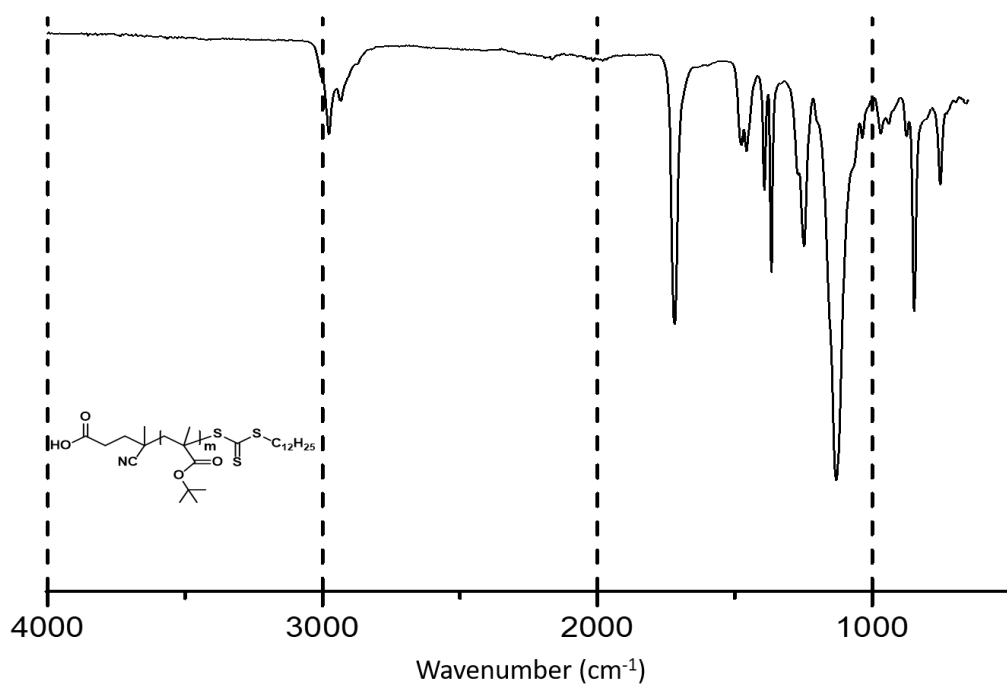


**Figure S5.** ATR-IR spectrum of PtBMA macro-CTA at 25 °C.

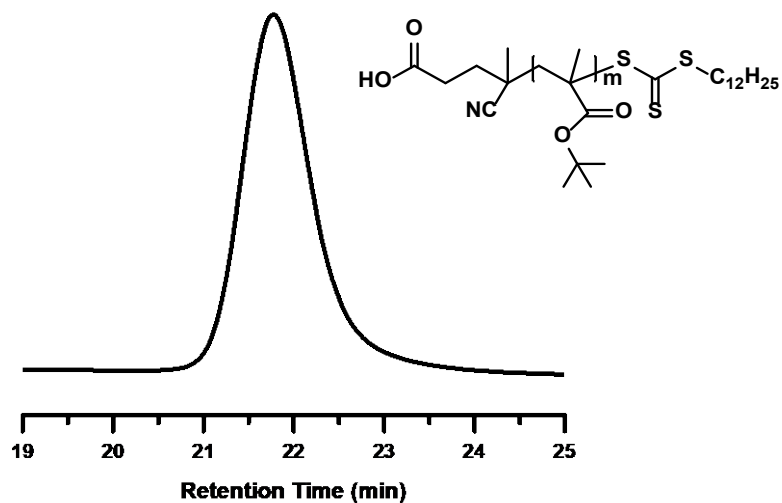


**Figure S6.** SEC-RI trace (THF mobile phase, 25 °C) of PtBMA macro-CTA ( $M_n = 51.0 \text{ kg mol}^{-1}$ ,  $\bar{D} = 1.04$ ) determined by MALS using a  $d\eta/dc = 0.065 \text{ mL/g}$ .

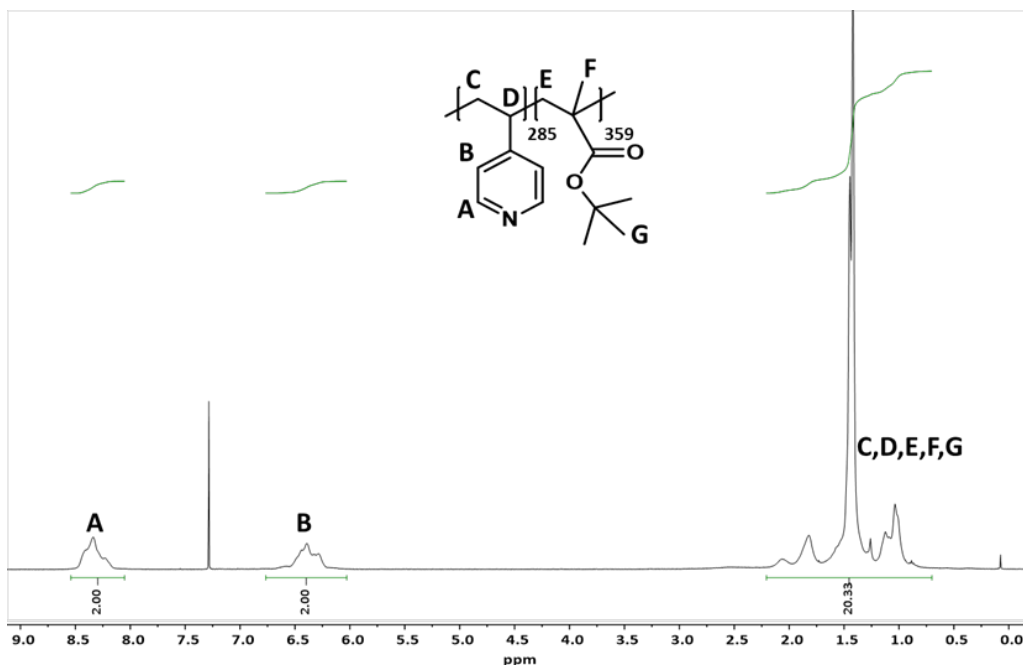


**Figure S7.** <sup>1</sup>H NMR (CDCl<sub>3</sub>, 25 °C) showing the integration ratios for P4VP-*b*-PtBMA used for determining molar ratios of each diblock copolymer segment.

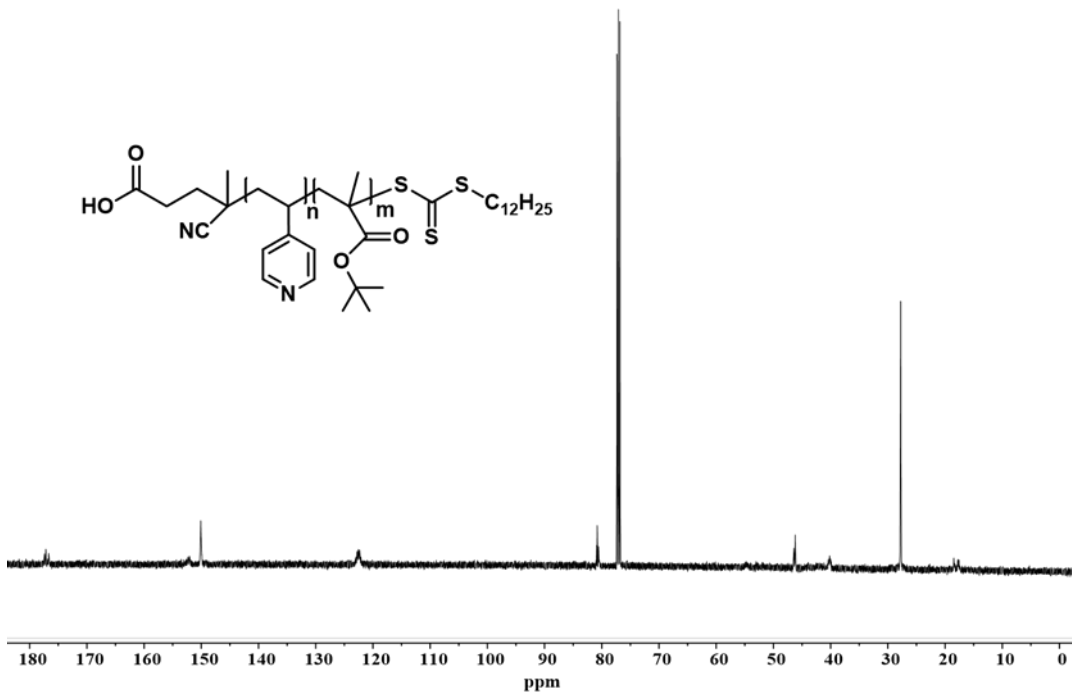


**Figure S8.** <sup>13</sup>C NMR (CDCl<sub>3</sub>, 25 °C, 125 MHz) of PtBMA-*b*-P4VP.

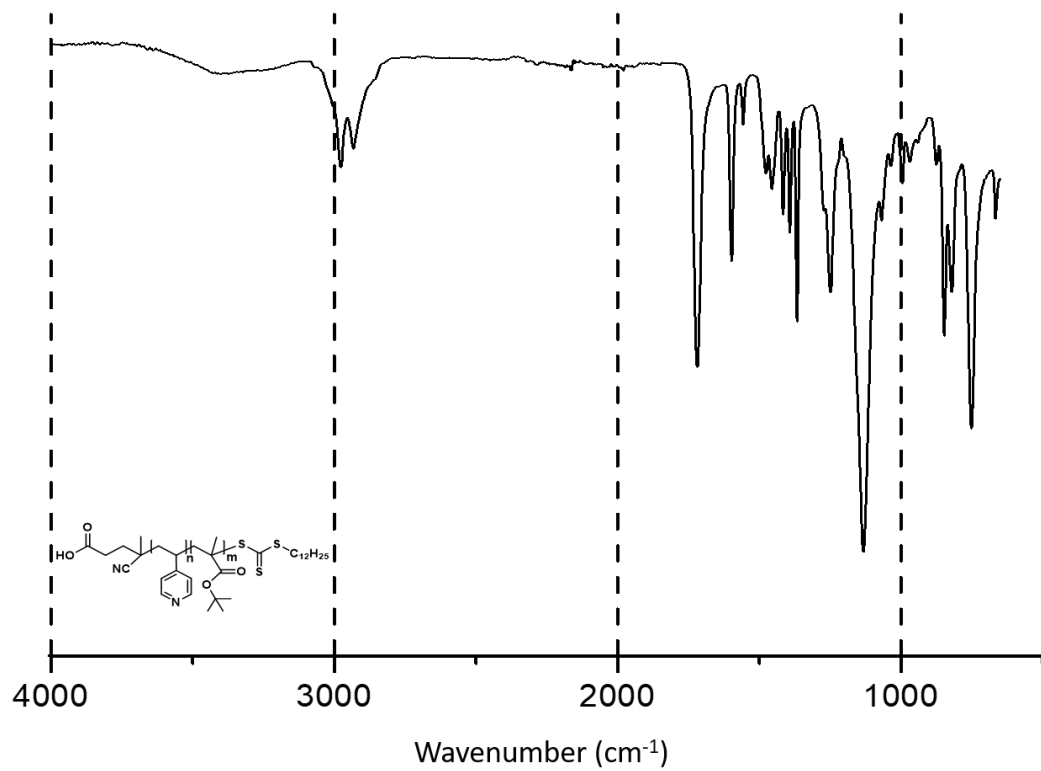


**Figure S9.** ATR-IR spectrum of PtBMA-*b*-P4VP at 25 °C.

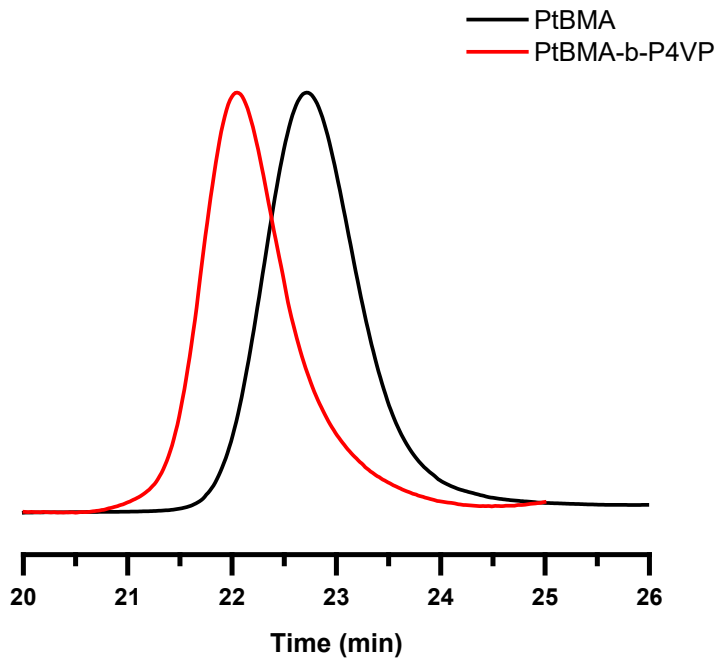


**Figure S10.** SEC-RI overlay trace (THF mobile phase, 25 °C) of PtBMA (black) and PtBMA-*b*-P4VP (red).

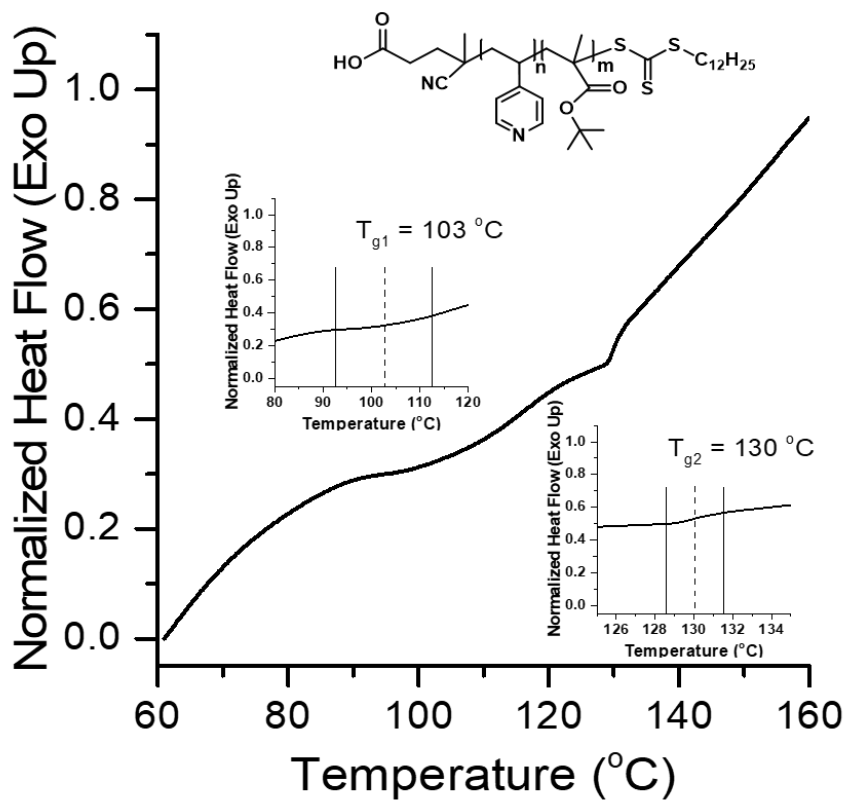


**Figure S11.** DSC thermogram of PtBMA-*b*-P4VP (exo up). Samples were cycled from 40 °C to 165 °C at a rate of 10 °C min<sup>-1</sup> under N<sub>2</sub> and the data shown was taken upon the 2<sup>nd</sup> heating.

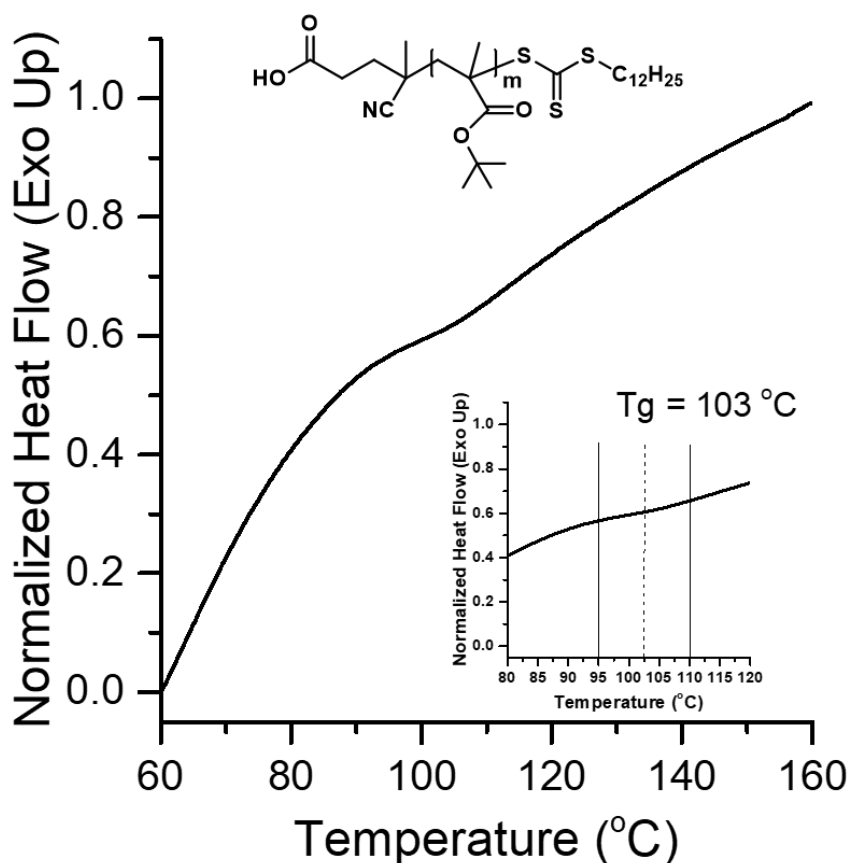


**Figure S12.** DSC thermogram of PtBMA macro-CTA (exo up). Samples were cycled from 40 °C to 165 °C at a rate of 10 °C min<sup>-1</sup> under N<sub>2</sub> and the data shown was taken upon the 2<sup>nd</sup> heating.

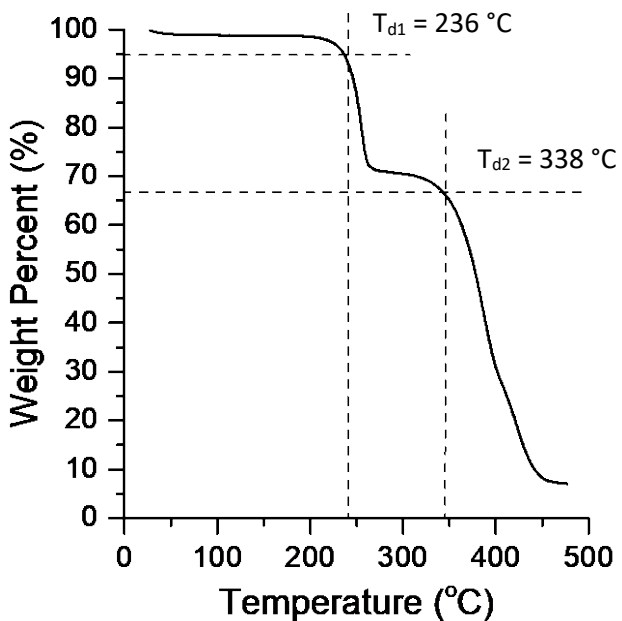


**Figure S13.** TGA thermogram of PtBMA-*b*-P4VP taken at a heating rate of  $10\text{ °C min}^{-1}$  under Ar. A two-step thermal decomposition is observed.

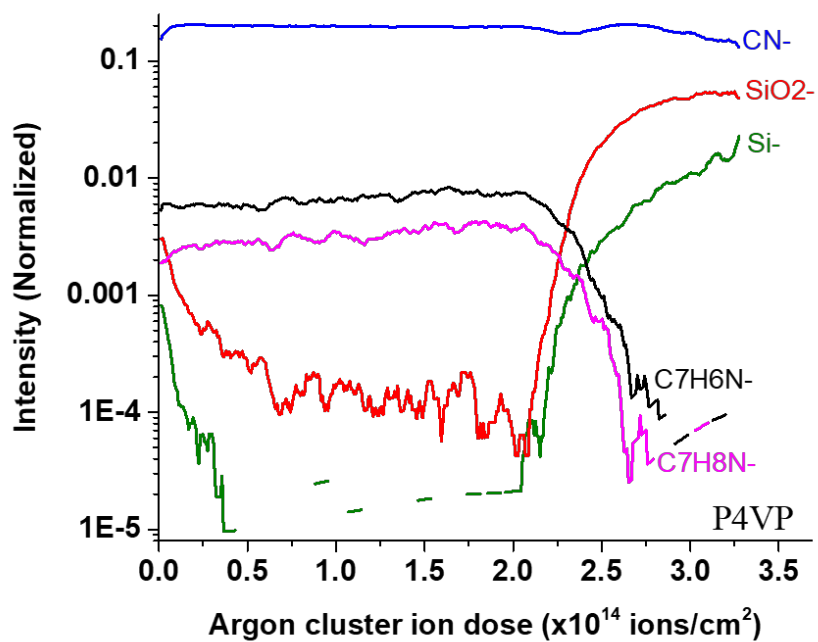


**Figure S14.** Normalized intensity of negative ion detection as a function of ion dose determined by ToF-SIMS in negative ion mode for P4VP homopolymer.

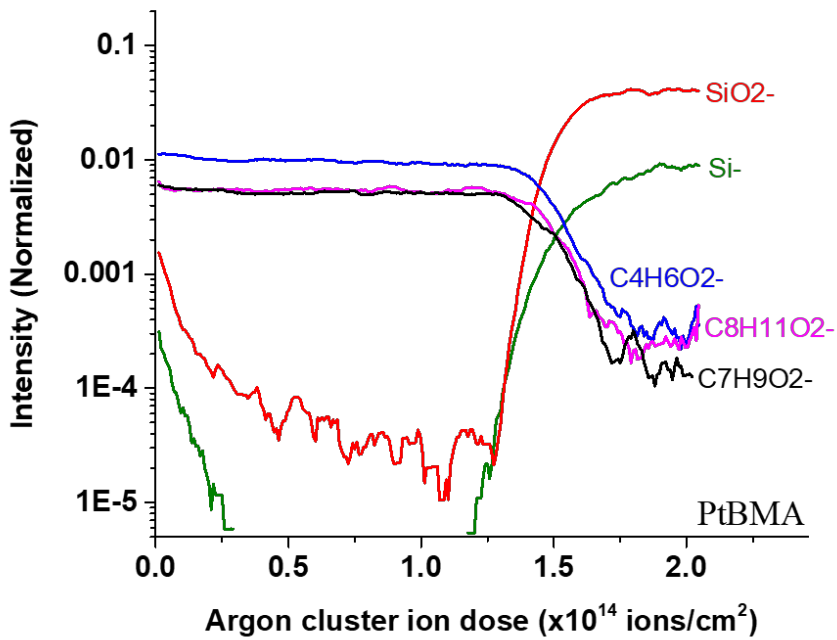


**Figure S15.** Normalized intensity of negative ion detection as a function of ion dose determined by ToF-SIMS in negative ion mode for PtBMA homopolymer

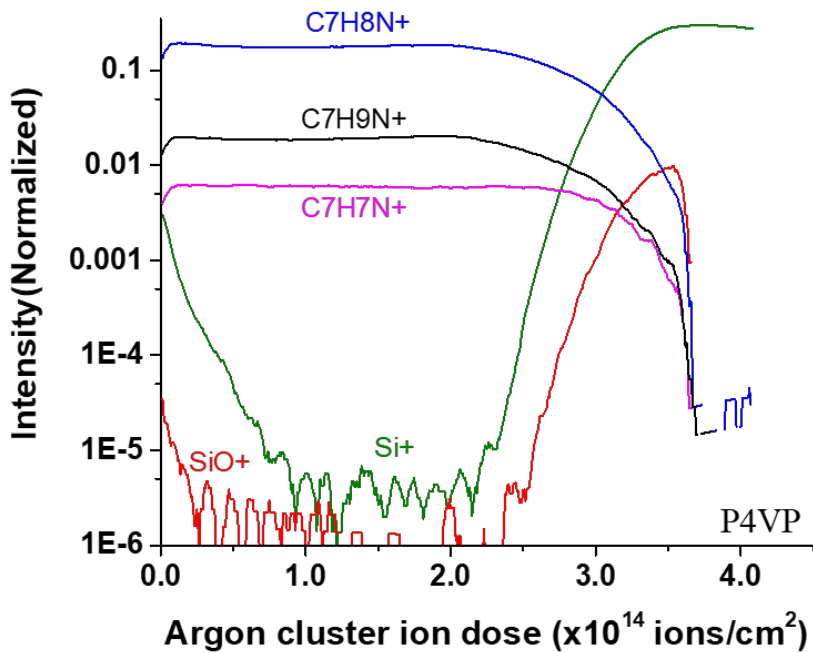


**Figure S16.** Normalized intensity of positive ion detection as a function of ion dose determined by ToF-SIMS in positive ion mode for P4VP homopolymer.

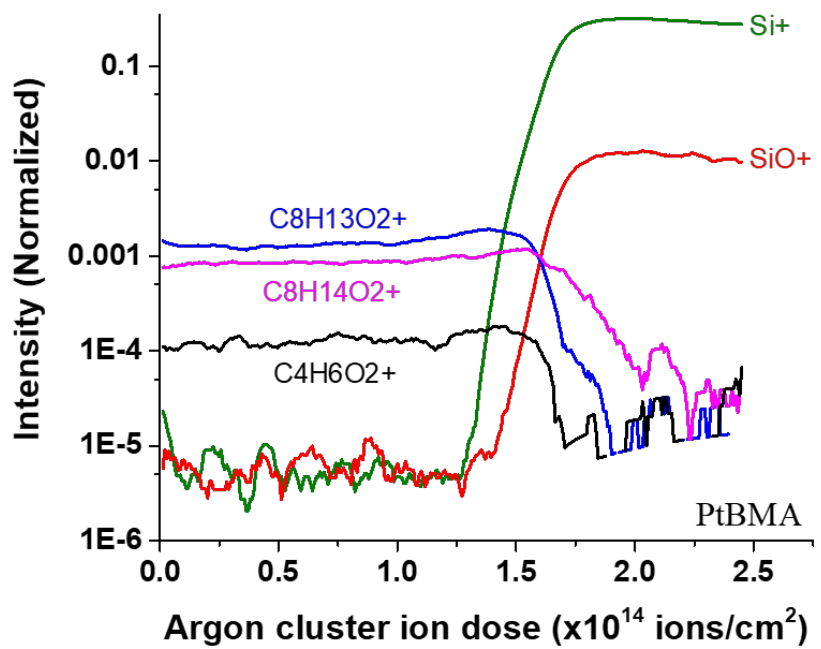


**Figure S17.** Normalized intensity of positive ion detection as a function of ion dose determined by ToF-SIMS in positive ion mode of PtBMA homopolymer.

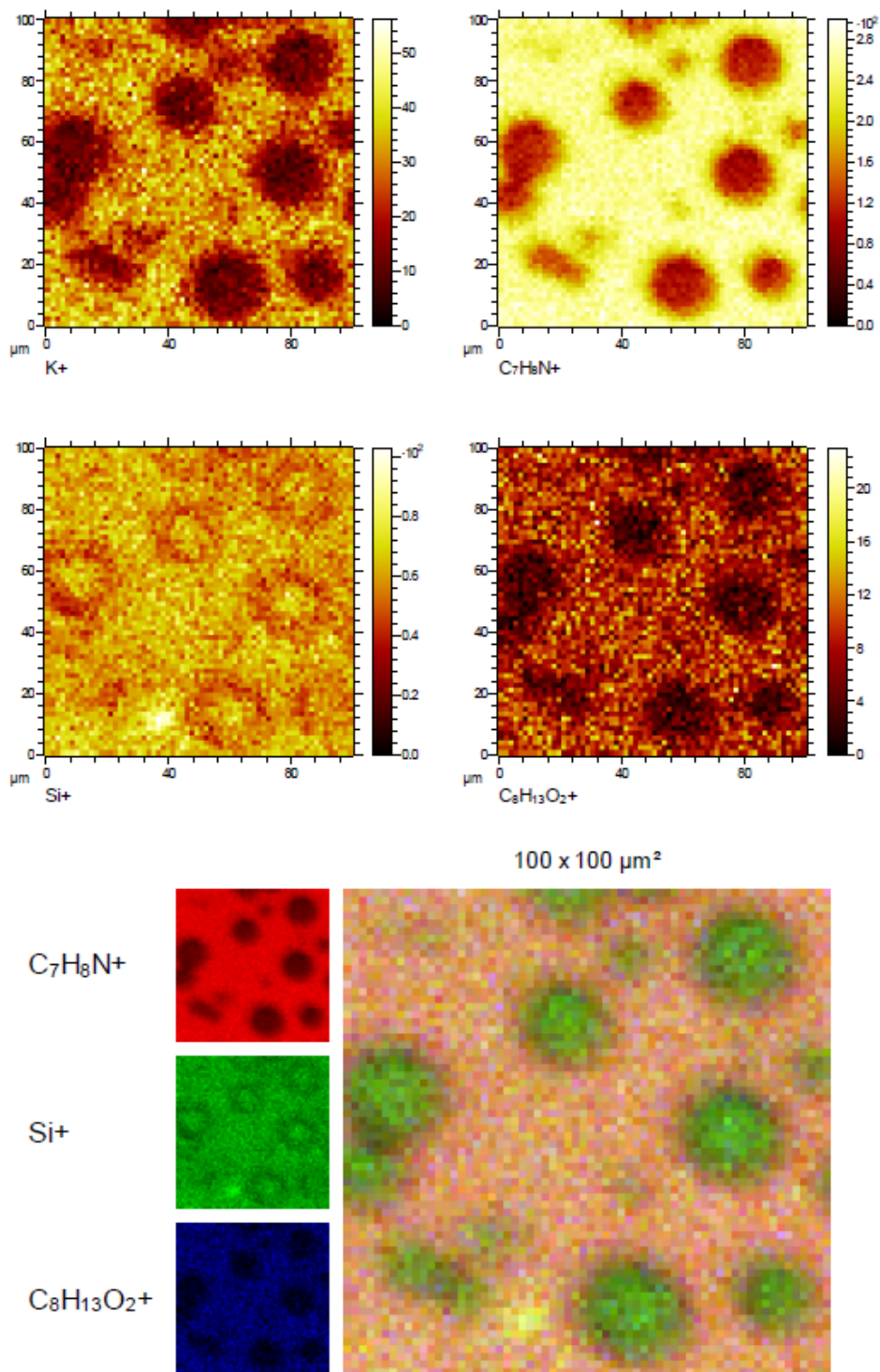


**Figure S18.** ToF-SIMS imaging of dewetted film **VP-MA(12-4)**. The characteristic ion images, here,  $C_7H_8N^+$  (red) for P4VP and  $C_8H_{13}O_2^+$  (blue) for PtBMA described a relatively homogeneous composition in the region without dewetting when the  $Si^+$  ion image displays the substrate in the bottom of the pits.

**Description and images of custom-built glassware apparatus for treatment of thin films with HCl vapor.**

A glass vial insert serves as the HCl reservoir which is housed within a pressure vessel that can be sealed with a PTFE cap and Viton o-ring (left picture). Another glass insert rests at the top of the pressure vessel and serves as a stage for the substrates to rest on (right picture). This glass insert has a bore in the center to allow HCl vapor exposure from the reservoir below.

